Chemical Physics Letters 774 (2021) 138631

Contents lists available at ScienceDirect

Chemical Physics Letters

journal homepage: www.elsevier.com/locate/cplett

Research paper

Ionization energy and thermochemistry of CF_2Cl_2 determined from threshold photoelectron spectroscopy

Hanhui Zhang [a,1], Tongpo Yu [a,1], Xiangkun Wu [a], Yan Chen [a,b], Baokun Shan [a], Xiaoguo Zhou [a,*], Xinhua Dai [b,*], Shilin Liu [a]

[a] Hefei National Laboratory for Physical Sciences at the Microscale, Department of Chemical Physics, University of Science and Technology of China, Hefei 230026, China

[b] National Institute of Metrology, Beijing 100013, China

ARTICLE INFO

Keywords:
Photoionization
Photoelectron spectroscopy
Franck-Condon factor
Adiabatic ionization energy
Enthalpy of formation

ABSTRACT

In this work, we performed a joint study of threshold photoelectron spectroscopy and density functional calculations on photoionization of CF_2Cl_2. Using the optimized geometries and vibrational frequencies of the CF_2Cl_2 neutral and cation in ground state at the ωB97XD/cc-pVTZ level, the Franck-Condon simulation was performed for the X^2B_2 band. Based on the great agreements between the experimental and simulated spectra, the observed vibrational progressions of the $CF_2Cl_2(X^1A_1) \rightarrow CF_2Cl_2^+(X^2B_2)$ transition are well assigned, leading to a corrected adiabatic ionization energy of 11.565 ± 0.010 eV. The enthalpies of formation and C-Cl bond energies of CF_2Cl_2 neutral and cation are then calculated, respectively.

1. Introduction

Dichlorodifluoromethane (CF_2Cl_2), commonly referred to as Freon 12, has been widely applied as refrigerant, aerosol propellant, plasma-processing agent and so on. Notably, CF_2Cl_2 plays a major role in depleting ozone layer in the stratosphere [1–3], as it can undergo dissociation by solar ultra-violet (UV) light to yield halogen atoms, especially the Cl atom [4–9]. Hence, the electronic structure and photodissociation of CF_2Cl_2, as well as its some analogues [10–13], have drawn extensive attentions. In comparison to the neutral molecule, investigations on the $CF_2Cl_2^+$ dissociation are limited, although the dissociative photoionization of CF_2Cl_2 under the action of vacuum UV (VUV) photons in ionosphere is also an important source of halogen atoms. Thus, an in-depth understanding of the dissociation of $CF_2Cl_2^+$ cation is worthy of greater concerns.

As fundamental parameters, ionization energy and vibrational frequencies are crucial to study molecular structures. Moreover, those accurate values are also essential for correctly modeling the related physics and chemistry. In past decades, for obtaining these accurate values of the CF_2Cl_2 neutral and cation, many experimental approaches were applied, *e.g.* electron-impact mass spectrometry (EI-MS) [9], photoionization mass spectrometry (PI-MS) [6,7], photoelectron spectroscopy (PES) [14–17], electron momentum spectroscopy (EMS) [18,19], VUV absorption and fluorescence spectroscopy [20], and threshold photoelectron-photoion coincidence (TPEPICO) spectroscopy [5]. Moreover, several theoretical methods were also performed to calculate geometries, vibrational frequencies, and dissociation limits of $CF_2Cl_2^+$ cation, for example, Hartree-Fock (HF) [21], multireference configuration interaction (MRCI) [22], and complete active space self-consistent field (CASSCF) and multi-configuration second-order perturbation theory (CASPT2) [23,24]. Table 1 summarizes the adiabatic ionization energies (AIEs) reported in experimental and theoretical studies. It is worth noting that these data show a large bias in different measurements.

Watanabe, Nakayama, and Mottl first reported ionization energies of about three hundred molecules including CF_2Cl_2 in a photoionization study without mass analysis [26]. Using PI-MS, Ajello *et al.* [6] observed an AIE of 11.75 eV and an AP(CF_2Cl^+) of 11.99 eV in the photoionization efficiency curve of CF_2Cl_2. With the same approach, Jochims *et. al.* [7] reported an AIE of 11.75 eV and an AP(CF_2Cl^+) of 12.10 eV. Later, Sheng *et al.* [25] determined these two values as 11.84 ± 0.05 eV and 12.05 ± 0.10 eV from the photoionization efficiency curve with synchrotron light source. In 1993, Pradeep *et al.* measured PES of a CF_2Cl_2 molecular beam using He-I light, and obtained the AIE values of 11.734, 13.078,

* Corresponding authors.
E-mail addresses: xzhou@ustc.edu.cn (X. Zhou), daixh@nim.ac.cn (X. Dai).
[1] H. Zhang and T. Yu contributed equally to this work.

https://doi.org/10.1016/j.cplett.2021.138631
Received 9 March 2021; Received in revised form 8 April 2021; Accepted 9 April 2021
Available online 20 April 2021

Table 1
Adiabatic ionization energy (AIE, eV) of CF_2Cl_2 reported in experimental and theoretical studies.

	Expt.	Theo.
PI-MS from Ref. [6]	11.75	
PI-MS from Ref. [7]	11.75	
PI-MS from Ref. [25]	11.84 ± 0.05	
PES from Ref. [14]	11.734	
TPES/TPEPICO, this work	11.565 ± 0.010	
HF from Ref. [21]		11.66
G2(MP2) from Ref. [25]		11.81
B3LYP/6–311++G(d,p), this work		11.63
M06-2X/cc-pVTZ, this work		11.72
ωB97XD/cc-pVTZ, this work		11.53

and 14.126 eV for the X, B and D ionic states, respectively [14]. Vibrational frequencies of the ν_3^+ and ν_4^+ modes for the X state, the ν_1^+ and ν_4^+ modes for the B state, and the ν_3^+ mode for the D state, were also achieved based on their vibrational analyses, where these four modes were all total symmetric. The vertical ionization energies (VIEs) are reported to be 12.28, 12.55, 13.14, 13.45, and 14.41 eV for the five lowest-lying states in the TPES of Seccombe *et al.* [5], very close to the PES result of Cvitas *et al.* [15]. Moreover, Cvitas *et al.* also reported the vibrational progressions of 280 cm^{-1} in X, 1090 cm^{-1} and 540 cm^{-1} in B, and 360 cm^{-1} in D states. In addition, the calculated AIE values are slightly inconsistent at the different level of theory, as shown in Table 1.

According to the AIE definition, it should be determined as the 0–0 band origin in experimental TPE spectra, or be calculated as the energy difference between the neutral and cation after zero-point energy corrections, each at its own optimized geometry. Therefore, a correct vibrational assignment is essentially crucial to determine an accurate AIE value in experiment, and provides a reasonable illumination for the previous disagreement. For this purpose, a new TPEPICO experiment has been conducted at the Hefei Light Source in this work. According to its multipurpose advantages [12,27], the TPE spectrum of CF_2Cl_2 is recorded with a relatively high resolution. Thanks to its specially designed ion optics, energetic electrons are efficiently suppressed in TPE spectra, providing more distinct vibrational structures. Thus, using this powerful experimental approach of photoionization, the AIE and VIE values of CF_2Cl_2 are reliably determined according to Franck-Condon factor (FCF) simulations with the aid of high-level quantum chemical calculations on the optimized geometries and vibrational frequencies of neutral and cation in ground state. Additionally, this joint study provides clues to evaluate energetics of the CF_2Cl_2 neutral and cation, like the enthalpy of formation and the C-Cl bond energy.

2. Experimental and theoretical methods

The TPE spectrum of CF_2Cl_2 in gas phase was measured using the TPEPICO velocity imaging spectrometer at the BL09U beamline in the Hefei Light Source, China. Details of the beamline and this apparatus have been described elsewhere [27], thus, only a brief introduction is given herein. The VUV photons from an undulator of an 800 MeV electron-storage ring were dispersed with a 6 m long monochromator. The present experiment was conducted in the photon energy range of 11.50–15.00 eV with a resolution power (E/ΔE) of ~ 2000 at 15 eV. More than 99% of the higher-order harmonic radiation was absorbed by a gas filter full of neon gas placed in front of the TPEPICO chamber. The absolute photon energy was calibrated using the well-known ionization energies of argon and neon [27], and the photon flux was detected with a silicon photodiode.

The CF_2Cl_2 (99.99%) gas mixed in helium (1/9 V/V) was introduced into the vacuum chamber through a 30 μm-diameter nozzle with a stagnation pressure of 1.2 atm. Then, the molecular beam was collimated by a 0.5 mm-diameter skimmer, then intersected with the VUV beam at 10 cm downstream from the nozzle. The backing pressures in the source and ionization chambers were 2×10^{-3} Pa and 2×10^{-5} Pa, respectively, with the molecular beam on. Photoelectrons and photoions were driven in opposite directions by a direct current extraction field (~15 V/cm). A specially designed ion optics was used to collect and map the velocity images of electrons and ions simultaneously [27]. A mask with a 1 mm-diameter hole and a concentric ring was placed in front of the electron detector at the end of flight tube. According to the velocity focus effect, the electrons with zero-kinetic energy could pass through the hole and were recognized as "threshold photoelectrons", meanwhile, the energetic electrons with an initial momentum towards the electron detector also could be detected to contribute the "false" threshold photoelectrons. Since those energetic electrons with a perpendicular momentum would partially pass the ring of the mask, their intensity were used to subtract this contamination in TPE spectra by those "false" threshold photoelectrons, as described previously [28]. Additionally, using photoelectrons to trigger time-of-flight (TOF) measurements of ions, the TPEPICO mass spectrum was recorded.

To interpret the TPE spectrum of CF_2Cl_2, geometry optimizations and vibrational frequency analyses of the CF_2Cl_2 neutral and cation were performed with the density functional theory (DFT) using the cc-pVTZ basis set. To evaluate accuracies of theoretical levels, two high-level DFT methods were applied, ωB97XD [29] and M06-2X [30], and compared with the previous *ab initio* calculation results like HF [21], MRCI [22], and CASSCF and CASPT2 [23,24]. Using the optimized geometries, the AIE value was calculated with ZPE corrections.

Based on the optimized geometries, harmonic frequencies, and normal-mode vectors for $CF_2Cl_2(X^1A_1)$ and $CF_2Cl_2^+(X^2B_2)$, the Franck-Condon (FC) factors calculations were carried out as the overlaps between initial and target vibrational states in a harmonic approximation using the ezSpectrum program [31]. Then, the TPE spectrum of $CF_2Cl_2^+(X^2B_2)$ was simulated with a certain full width at half maximum (FWHM), in which the calculated AIE value was slightly shifted to greatly match the experimental spectrum. It is worth noting that the comparison between the simulated and experimental spectra was mainly done at the rising edge, since the non-harmonic effects of vibrational frequencies would lead to some obvious deviations at the high-energy side. As a result, the observed vibrational progressions of this photoionization electronic transition of $CF_2Cl_2(X^1A_1) \rightarrow CF_2Cl_2^+(X^2B_2)$ were reliably assigned. Therefore, an accurate AIE value was derived from the vibrational assignment as the 0–0 band origin. All the quantum chemical computations were performed with the Gaussian 16 program package [32].

3. Results and discussion

3.1. Threshold photoelectron spectrum of CF_2Cl_2

In a TPE spectrum measurement, threshold photoelectrons are produced and collected at various photon energies with a tunable VUV light source, and the vibrational peak intensity is proportional to the product of the FC factors and the electronic transition cross sections from neutral to cation. Besides, the auto-ionization of Rydberg states always accompanies with those direct ionization processes, leading to a certain contamination in TPE spectra, especially in a FC gap between adjacent ionic states. In comparison to TPE spectra, photoelectron spectra are usually measured using a fixed energy light source like He-I, and the electron energy is analyzed with a dispersive energy analyzer. Thus, the auto-ionization of Rydberg states is excluded in the spectra due to different transition cross sections. Therefore, the original TPE spectrum recorded in our experiment was normalized using the measured photon flux, and then modified according to the spectral intensities in FC gaps in the previous He-I photoelectron spectra [14,15]. Fig. 1 shows the revised TPE spectrum of CF_2Cl_2 in the photon energy range of 11.50–12.80 eV, with a step size of 5 meV.

Two electronic bands with different vibrational structures were observed in Fig. 1. The overall peak positions and relative intensities of

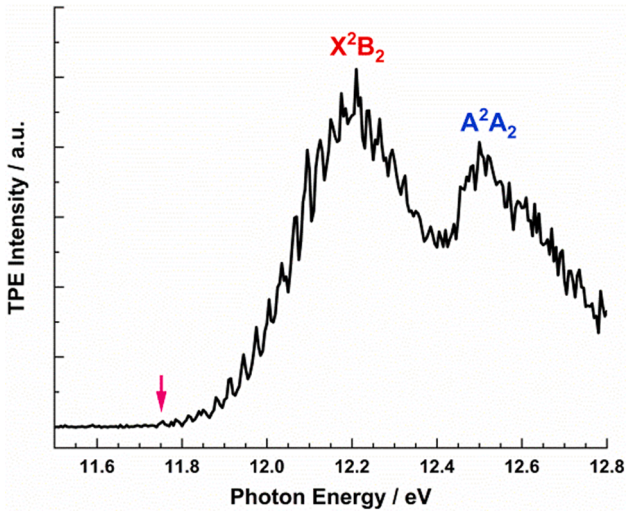

Fig. 1. Threshold photoelectron spectrum of CF_2Cl_2 in the photon energy range of 11.50–12.80 eV, with a step size of 5 meV. The onset peak was labeled with a pink arrow.

the two bands are generally consistent with the Seccombe *et al.*'s TPE spectrum [5], but more abundant details of vibrational structures are recorded, providing more clues for determining adiabatic ionization energies and vibrational frequencies as the following discussions. Moreover, the major spectral properties also agree with the He-I photoelectron spectra [14,15], regardless of resonance positions and relative intensities. According to the conclusions of TPE [9] and photoelectron [14,15] spectra, these two bands are readily assigned to the X^2B_2 and A^2A_2 states of $CF_2Cl_2^+$ cation, respectively.

As shown in Fig. 1, the X^2B_2 band starts from ~ 11.75 eV and overlaps with the A^2A_2 band at ~ 12.45 eV. A well-resolved vibrational progress with an interval of ~ 0.035 eV can be observed at the rising edge of X^2B_2, while the peaks at the higher-energy side show slightly wider profiles. Table 2 lists those discernible peak positions of X^2B_2. Apparently, there is a large energy difference of 0.455 eV between the onset (the peak noted with a pink arrow in Fig. 1) and the peak maximum (at 12.210 eV), indicative of a serious geometry change in photoionization. In this case, it is difficult to simply assign this threshold onset to the X^2B_2 band origin (*i.e.* AIE), due to the unfavorable FC factor of band origin (probably too weak to be detected in experiment).

Table 2
Vibrational peak positions and their assignments of threshold photoelectron spectrum corresponding to the transitions of $CF_2Cl_2(X^1A_1, v = 0) \rightarrow CF_2Cl_2^+(X^2B_2, \nu^+)$.

Peak positions /eV	Energy relative to the first peak /cm^{-1}	assignment ($\nu_1^+,\nu_2^+,\nu_3^+,\nu_4^+$)	Peak positions /eV	Energy relative to the first peak /cm^{-1}	assignment ($\nu_1^+,\nu_2^+,\nu_3^+,\nu_4^+$)
11.755	0	(0,0,0,5)	12.175	3388	(0,0,0,19)
11.785	242	(0,0,0,6)			& (1,0,0,14)
11.815	484	(0,0,0,7)	12.210	3670	(1,0,0,15)
11.850	766	(0,0,0,8)			& (0,0,0,20)
11.880	1008	(0,0,0,9)	12.240	3912	(1,0,0,16)
11.915	1290	(0,0,0,10)			& (0,0,0,21)
11.945	1532	(0,0,0,11)	12.265	4113	(1,0,0,17)
11.975	1774	(0,0,0,12)			& (0,0,0,22)
12.005	2016	(0,0,0,13)	12.295	4355	(1,0,0,18)
12.035	2258	(0,0,0,14)			& (0,0,0,23)
12.070	2541	(0,0,0,15)	12.325	4597	(1,0,0,19)
12.095	2742	(0,0,0,16)			& (0,0,0,24)
12.125	2984	(0,0,0,17)	12.350	4799	(1,0,0,20)
12.150	3186	(0,0,0,18)			& (0,0,0,25)

Moreover, the lowest fragmentation channel for dissociative photoionization of CF_2Cl_2 is to produce $CF_2Cl^+(X^1A_1)$ + $Cl(^2P)$, with the appearance energy of ~ 12.0 eV, while the second dissociation limit of $CFCl_2^+(X^1A_1)$ + $F(^2P)$ was measured to be much higher and beyond the present photon energy range [5–9]. Consequently, except for the onset region, the fragmentation of $CF_2Cl_2^+$ is open in the whole energy range of X^2B_2, resulting in the broadening of vibrational peaks in some degree. This broadening becomes more obvious in the A^2A_2 band, where a wide and intense peak is located at 12.500 eV, overlapping with a slightly weaker shoulder. There are no vibrational peaks able to be obviously discerned for the A^2A_2 band in Fig. 1. The whole A^2A_2 band starts from ~ 12.43 eV, and generally agrees with the previous spectra [5,14,15]. Such wide vibrational peak profiles strongly indicate the dissociative character of A^2A_2 in FC region.

3.2. TPEPICO time-of-flight spectrum

Although the CASSCF and CASPT2 calculations confirmed the local minimum property of both X^2B_2 and A^2A_2 states [23,24], $CF_2Cl_2^+$ parent ions were hardly observed in the previous experiments [5–9]. This contradiction might be due to their relatively shallow wells in comparison to the $CF_2Cl_2^+$ internal energy yielded in the FC photoionization. Therefore, to validate the existence of $CF_2Cl_2^+$ cations, the TPEPICO TOF mass spectra were measured at various photon energies, especially near the threshold onset. Fig. 2 shows the recorded mass spectra at seven representative photon energies, *e.g.* 11.915, 11.945, 11.975, 12.155, and 12.270 eV for the X^2B_2 band, and 12.525 and 12.670 eV for A^2A_2, respectively.

At the photon energy below 12.155 eV, the $CF_2^{35}Cl^{35}Cl^+$ (*m/z* 120) and $CF_2^{35}Cl^{37}Cl^+$ (*m/z* 122) parent ions were observed at 22.56 and 22.75 μs, respectively, in Fig. 2, with nearly intensity ratio of 3:1 and a FWHM of ~ 59 ns, whereas the $CF_2^{37}Cl^{37}Cl^+$ (*m/z* 124) cation was not detected due to its considerably low abundance. As we expected, the parent ions soon disappeared with the increase of photon energy. The CF_2Cl^+ fragment ions (*m/z* 85 for $CF_2^{35}Cl^+$ and *m/z* 87 for $CF_2^{37}Cl^+$), which were located at 18.96 and 19.19 μs, respectively, began to appear at 11.945 eV. Due to kinetic energy release in dissociation, the TOF distribution of CF_2Cl^+ was much broadened in contrast to that of the parent ion. Their relative intensities agree with the natural isotopic abundance of chloride atom (^{35}Cl:^{37}Cl = 3:1). Our results undoubtedly verify that the X^2B_2 ionic state is stable with a shallow well indeed. It is

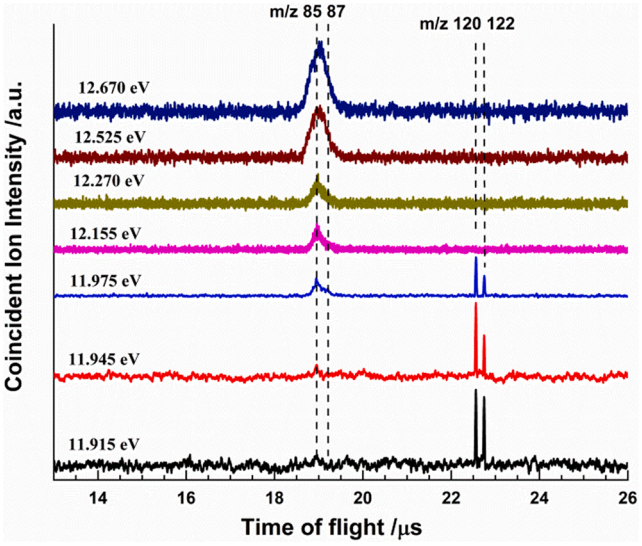

Fig. 2. TPEPICO time-of-flight mass spectra for the dissociative photoionization of CF_2Cl_2 at a few representative photon energies, *e.g.*, 11.915, 11.945, 11.975, 12.155, 12.270, 12.525, and 12.670 eV, respectively.

worth noting that the elusive parent ions solely were observed in a narrow range of 11.915–11.975 eV (in Fig. 2), where these three energies corresponded to the adjacent vibrational peaks in Fig. 1. Although the AIE value is probably located at a lower photon energy, the further detection below 11.915 eV is indeed limited by the insufficient instrumental sensitivity. Moreover, this appreciably narrow observable range of the parent ion $CF_2Cl_2^+$, on the other hand, impedes the plotting of the fractional abundances of the parent and fragment ions in a breakdown diagram, but we can directly determine the appearance energy, AP (CF_2Cl^+/CF_2Cl_2), as 11.945 ± 0.010 eV. Thanks to the advantages of molecular beam in the present measurement and more discernible vibrational structure in Fig. 1, our AP(CF_2Cl^+) value is reliable enough within its uncertainty, which is greatly consistent with the Seccombe *et al.*'s value (11.95 ± 0.05 eV) [5] and the other previous data (11.96 ± 0.03 eV [8], 12.05 ± 0.10 eV [25]). Additionally, no parent ions were residual in the energy range of A^2A_2, validating its dissociative feature in the FC photoionization. The TOF profile of CF_2Cl^+ maintains a same shape with a gradually increased width.

3.3. Geometry, energy and vibrational frequencies of $CF_2Cl_2^+(X^2B_2)$

In previous studies [14,25], the AIE value of CF_2Cl_2 was usually obtained by adding the instrumental resolution to the electron binding energy at the crossing point between the onset of spectral band and the baseline in TPE or photoionization efficiency spectra. However, in principle the AIE value should be exactly located at the 0–0 transition. Apparently, due to a large geometry change upon photoionization, it is difficult to directly determine AIE of the X^2B_2 state in Fig. 1, due to lack of vibrational assignments (the 0–0 transition might be too weak to be observed). By contrast, measuring VIE is much easier, which is just located at the peak maximum in TPE spectra. In Fig. 1, the VIE values of the X^2B_2 and A^2A_2 states are readily determined to be 12.210 and 12.500 eV, respectively, which are in general agreement with the previous data [5,15].

To achieve a reliable assignment of TPE spectra, the FC simulation spectrum is the best solution, in which molecualr geometries and harmonic vibratioanl freqeuncies of neutral and cation are necessary. Fig. 3 shows the optimized geometries of the CF_2Cl_2 neutral and its cation in the ground state at the ωB97XD/cc-pVTZ level of theory. The optimized geometries at the different levels of theory are generally consistent as shown in Table S1 of the supporting information, *e.g.* M06-2X/cc-pVTZ, HF/MIDI-4 [21], CASSCF/ANO-L and CASPT2//ANO-L [23]. As shown in Fig. 3, the two C-F bond lengths are shorten from 1.324 Å in neutral to 1.279 Å in cation, while the other C-Cl bond are elongated to 1.808 Å upon ionization, indicative of the weaker C-Cl interaction in the cation. Actually, this weakening of C-Cl bonds leads to the less stable cation and the lower dissociation limit, as indicated in experiments. Besides the bond length changes, the bond angle of Cl-C-Cl is dramatically decreased from 111.4° in neutral to 89.3° in cation. These geometrical variations in the photoionization process strongly indicate that the scissoring mode of CCl_2 group (ν_4^+ in Fig. 4) predominates, accompanying with considerable excitations of C-F and C-Cl symmetric stretching. More importantly, this appreciable geometrical distortion would result in a very small FC factor for the 0–0 transition, accounting for the gentle rising edge of the X^2B_2 band in TPE spectrum and the large difference between AIE and VIE (*c.a.* 0.6 eV).

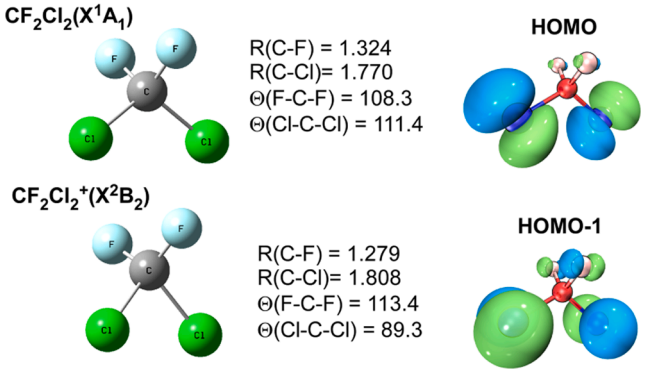

Fig. 3. Optimized geometries of the CF_2Cl_2 neutral and its cation in the ground state at the ωB97XD/cc-pVTZ level of theory, as well as the HOMO and HOMO-1 orbitals of neutral, where the bond lengths (R) are in unit of Å and the bond angles (Θ) are in degree.

In addition, as listed in Fig. 3, the two highest occupied molecular orbitals (HOMO and HOMO-1) of the neutral CF_2Cl_2 molecule predominantly consist of the *p* orbitals of chlorine atoms. Once an electron is removed from them, the cation in the X^2B_2 or A^2A_2 states is produced. Thus, the corresponding electron density distribution of molecular orbital implies that the electron being removed from an arbitrary halogen will indeed strengthen repulsive interaction between the specific halogen and the carbon atom, thus inducing the cleavage of C-Cl bond, which reasonably interprets the dissociative photoionization of $CF_2Cl_2^+(X^2B_2)$ cation.[5]

Besides the ν_4^+ vibrational mode, there are the other three total symmetric modes which can probably be excited in photoionization, while all asymmetric vibrational modes are forbidden [14–16,21]. Fig. 4 lists all these four total symmetric vibrational modes. Besides the ν_4^+ mode mentioned above, the ν_3^+ mode is dominantly contributed by combination of the C-F-C scissoring and the C-Cl stretching, while the ν_2^+ and ν_1^+ modes primarily correspond to the carbon atom motion along the C_{2v} symmetric axis of molecule, combined with the C-F bond scissoring or shrinking.

Table 3 summarizes the calculated frequencies of these four vibrational modes at several different levels. In general, the HF and CASSCF levels predict the higher frequencies than those of M06-2X and ωB97XD by about 8%, although the optimized structures are similar. Compared with the previously reported vibrational frequencies in experiment [14], both DFT calculations (M06-2X and ωB97XD) show the better agreement. Therefore, the FC factor calculation and simulation of TPE spectrum were performed using the ωB97XD data in the following section.

3.4. Franck-Condon simulated TPE spectrum

Using the optimized geometries, harmonic frequencies, and normal-mode vectors for the CF_2Cl_2 neutral and cation in the ground state, the FC factors were calculated and shown as the colorized sticks in Fig. 5. It is worth noting that less anharmonic effects are included in the lower energy side of TPE spectrum, thus the FC simulation was paid more attention to the rising-edge part in TPE spectrum according to the harmonic approximation in FC factor calculations. Thus, based on the calculated FC factors, the TPE spectrum was simulated with a FWHM of 200 meV at room temperature, and was compared with the experimental one, considering the instrumental resolution and predissociative broadening of vibrational peaks.

Fig. 5 plots the simulated TPE spectrum for the transition of $CF_2Cl_2(X^1A_1) \rightarrow CF_2Cl_2^+(X^2B_2)$, in comparison to the experimental one. The simulated band is apparently wider than the experimental one due to ignoring anharmonic effects, but the whole band and vibrational peak profiles exactly agree with each other. As shown in Fig. 5, the excitations of three vibrational modes, ν_1^+, ν_2^+, and ν_4^+, are dominantly involved in this X^2B_2 band as suggested by the geometrical variation from neutral to cation, thus, three series of vibrational progressions, $0 \rightarrow n\nu_4^+$, $0 \rightarrow (1\nu_1^+, n\nu_4^+)$, and $0 \rightarrow (1\nu_2^+, n\nu_4^+)$ (n = 5–28), are observed in Fig. 5. Among them, the sole vibrational excitation of the ν_4^+ mode almost covers the whole band, and the strongest transition is located at n = 16. In comparison to the other combination vibrational bands of $0 \rightarrow (1\nu_1^+, n\nu_4^+)$ and $0 \rightarrow (1\nu_2^+, n\nu_4^+)$, the rising edge of the X^2B_2 band is almost entirely contributed by the $0 \rightarrow n\nu_4^+$ transitions as indicated in the red sticks of Fig. 5, thus providing a perfect candidate to validate our FC simulations. As shown in Fig. 5, an excellent agreement was obtained between the

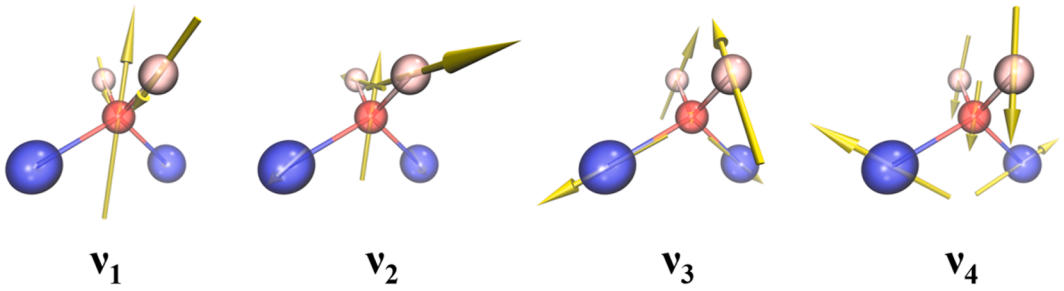

Fig. 4. The four total symmetric vibrational modes of the CF_2Cl_2 neutral and cation, where the yellow arrows represent the vibrational displacement vectors of atoms.

Table 3
Vibrational frequencies (cm^{-1}) of the total symmetric vibrational modes for the $CF_2Cl_2^+(X_2B_2)$ cation, calculated at the different quantum chemical levels of theory.

	Theo.				Expt.	
Mode	HF[a]	CASSCF[b]	M06-2X	ωB97XD	PES[c]	Present
ν_1^+	1322	1301	1235	1228	1204	1282
ν_2^+	753	733	710	705	–	–
ν_3^+	498	471	466	462	–	–
ν_4^+	303	283	277	270	266	283

a. from Ref. [21].
b. from Ref. [23].
c. from Ref. [14].

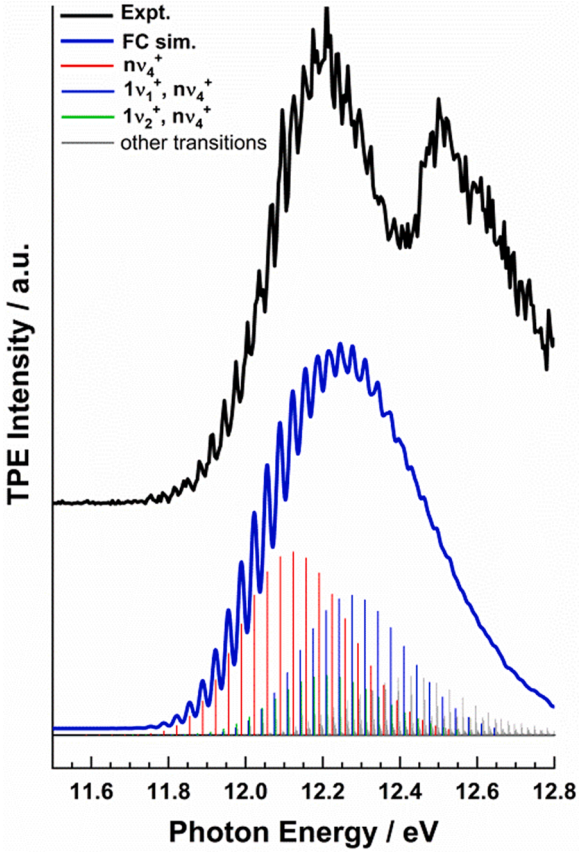

Fig. 5. Experimental and Franck-Condon simulated TPE spectra of CF_2Cl_2 in the X^2B_2 ionic state, using the optimized geometries, vibrational frequencies, normal coordinates calculated at the ωB97XD/cc-pVTZ level of theory. The red, blue, and green sticks correspond to the 0 → $n\nu_4^+$, 0→($1\nu_1^+$,$n\nu_4^+$), and 0→($1\nu_2^+$, $n\nu_4^+$) transitions, respectively.

experimental and simulated spectra in the low-energy side, by a slight shift of the calculated AIE. To our surprise, the experimental threshold onset (11.755 eV) just corresponds to an overtone excitation of 0 → $5\nu_4^+$, based on our FC simulation. The 0–0 band origin and the lower-energy transitions of 0 → $n\nu_4^+$ (n = 1–4) are too weak to be observed, due to such a large structural change in photoionization. Thus, thanks to the excellent agreement of the FC simulation at the rising edge (especially in the region of less than 12.0 eV photon energy), those vibrational peaks observed in experiment can be assigned and listed in Table 2. It is worth noting that the anharmonic effects should be not negligible for those high vibrational excitations, although our FC simulation with the harmonic approximation did not consider them. Hence, we manually adjusted those calculated high vibrational peak positions to match the experimental peaks as closely as possible. Then, using the assigned transitions of 0 → $n\nu_4^+$ (n = 5–16) in Table 2 (those have less influences from the other combination bands), the band origin of 0–0 transition is eventually determined to be 11.565 ± 0.005 eV, *i.e.* AIE, referring to the formula of vibrational state energy, $E_n = E_0 + \omega_e\left(n+\frac{1}{2}\right) - \omega_e\chi_e\left(n+\frac{1}{2}\right)^2$, in cm^{-1}, where ω_e and $\omega_e\chi_e$ are the vibrational frequency and the anharmonic parameter of the ν_4^+ mode. The ω_e and $\omega_e\chi_e$ are determined to be 283 and 1.44 cm^{-1}, respectively, which are considerably different from the values (266 and 12.1 cm^{-1}) suggested by Predeep and Shirley [14]. Since these previous values were simply derived from the energy intervals of peaks without reliable spectral assignments, we believe our ω_e and $\omega_e\chi_e$ values are more credible and firmly established. Furthermore, using the new vibrational assignments in Table 2, the AIE value of CF_2Cl_2 is corrected to be 11.565 ± 0.010 eV, which is obviously lower than those previous experimental data in Table 1, and greatly agree with our calculated values at the ωB97XD/cc-pVTZ level. The uncertainty of 0.010 eV comes from a combination error in the VUV energy resolution (ca. 7 meV) and the spectral fitting. In addition, the present assignments also provide a reasonable explanation for the inconsistence between theoretical and previously experimental data.

In addition to the dominant transition of 0 → $n\nu_4^+$ in the lower-energy side, the other two combination vibrational progressions of 0→($1\nu_1^+$, $n\nu_4^+$) and 0→($1\nu_2^+$,$n\nu_4^+$) have more significant contributions to the higher energy moiety of the X^2B_2 band, as shown in Fig. 5. The 0→($1\nu_1^+$,$n\nu_4^+$) transitions have approximately equivalent energies with the 0→($1\nu_2^+$,(n + 2)ν_4^+) ones but display stronger FC intensities. The most intense vibrational peak among this combination progression of 0→($1\nu_1^+$,$n\nu_4^+$) is calculated still at n = 16 (Fig. 5), which agrees with the sole 0 → $n\nu_4^+$ transitions. As listed in Table 2, seven discernible vibrational peaks in the high-energy side of X^2B_2 are inclined to be attributed to this combination progression. Moreover, the gap between the 0 → $n\nu_4^+$ peak and the adjacent 0→($1\nu_1^+$,(n − 5)ν_4^+) one is approximately 0.016 eV as indicated by the blue and red sticks in FC simulated spectrum, which is in general agreement with the energy interval of ~ 0.016 eV between the adjacent peaks of different vibrational progressions observed in the Predeep and Shirley's photoelectron spectra. [14]. This agreement

further verifys the reliability of the FC simulation and helps us to correct their vibrational assignments of the other progressions, such as 0→($2\nu_2^+$, $n\nu_4^+$). Taking this advantage, we can readily acquire the ν_1^+ value as 1282/1204 cm^{-1} in our/their experiments using $5\nu_4^+ - \nu_1^+ = 0.016$ eV. In addition, the other transitions, denoted with grey sticks in Fig. 5, predominantly contribute in relatively higher energy region. Since the spectrum in this region may include too many complicated combination vibrations and more serious anharmonic effects, the FC simulated spectrum in the harmonic approximation is not reliable enough to provide satisfying assignments, meanwhile, the overlapping from the A^2A_2 excited state further aggravates this uncertainty.

3.5. Enthalpies of formation and C-Cl bond energies of CF_2Cl_2 neutral and cation

Based on the present AIE of CF_2Cl_2 and the AP(CF_2Cl^+/CF_2Cl_2) values, we can easily calculate the C-Cl bonding energy of $CF_2Cl_2^+$ cation as BE(C-Cl in $CF_2Cl_2^+$) = AP(CF_2Cl^+/CF_2Cl_2) − AIE(CF_2Cl_2) = 11.945–11.565 = 0.380 ± 0.010 eV, which is larger than the Sheng *et al.*'s data [25]. In addition, using the reported $\Delta_fH^o_{298K}(CF_2Cl^+,g)$ of 549.5 ± 3.4 kJ·mol^{-1} [33] and $\Delta_fH^o_{298K}(Cl)$ = 121.302 ± 0.0011 kJ·mol^{-1} [34], the enthalpy of formation of $CF_2Cl_2^+$, $\Delta_fH^o_{298K}(CF_2Cl_2^+$, g), can be calculated as $\Delta_fH^o_{298K}(CF_2Cl_2^+,g) = \Delta_fH^o_{298K}(CF_2Cl^+$, g) + $\Delta_fH^o_{298K}(Cl)$ − BE(C-Cl in $CF_2Cl_2^+$) = 633.7 ± 4.4 kJ·mol^{-1}.

There are a few inconsistent AIE values of CF_2Cl free radical in literatures, *e.g.* 8.30 [35] and 9.0 ± 0.5 eV [36] in experiments, 8.41 eV at G2MP2 level [25] and 8.51 eV at G3X level [37]. Thus, we prefer to obtain it indirectly from thermochemistry. Using the early reported enthalpy of formation of CF_2Cl free radical, $\Delta_fH^o_{298K}(CF_2Cl,g)$ = –269.03 ± 8.37 kJ·mol^{-1} [38], AIE($CFCl_2$) can be calculated as $\Delta_fH^o_{298K}(CF_2Cl^+,g) - \Delta_fH^o_{298K}(CF_2Cl,g)$ = 549.5–(–269.03) = 818.5 ± 11.8 kJ·mol^{-1} = 8.48 ± 0.12 eV. Following this value, the C-Cl bonding energy of the neutral CF_2Cl_2 molecule is determined to be BE(C-Cl in CF_2Cl_2) = AP(CF_2Cl^+/CF_2Cl_2) -AIE(CF_2Cl) = 11.945–8.48 = 3.49 ± 0.13 eV.

Additionally, according to the unimolecular decomposition reaction of $CF_2Cl_2 \rightarrow CF_2Cl + Cl$, the C-Cl bonding energy of CF_2Cl_2, BE(C-Cl in CF_2Cl_2), can be calculated as the following equation

BE(C-Cl in CF_2Cl_2) = $\Delta_fH^o_{298K}(CF_2Cl,g)$ + $\Delta_fH^o_{298K}(Cl)$-$\Delta_fH^o_{298K}(CF_2Cl_2$, g).

In the ATcT database [34], $\Delta_fH^o_{298K}(CF_2Cl_2$, g) is reported to be –493.65 ± 0.67 kJ·mol^{-1}. Thus, BE(C-Cl in CF_2Cl_2) is equal to 345.92 ± 9.04 kJ·mol^{-1}, *i.e.* 3.59 ± 0.09 eV, which generally agrees with the value of 3.64 ± 0.10 eV reported by Sheng *et al.* [25] and the derived value (3.69 ± 0.04 eV) from the reaction of $CF_2Cl_2(+M) \rightarrow CF_2Cl + Cl$ (+M) [39]. In comparison to those of the other chlorofluorocarbons, *e.g.* $CFCl_3$ (BE = 3.32 ± 0.02 eV from RRKM calculation [40], 3.44 ± 0.19 eV from TPEPICO measurement [41]), and CF_3Cl (BE = 3.73 ± 0.01 eV from TPEPICO experiment [10], 3.86 ± 0.07 eV from RRKM calculation [42]), the C-Cl bonding energy exhibits a monotonically increasing sequence along $CFCl_3 \rightarrow CF_2Cl_2 \rightarrow CF_3Cl$, which is consistent with the fact that the more fluorine atoms, the weaker C-Cl bond in chlorofluorocarbons is, due to the stronger electronegativity of fluorine atom.

4. Conclusion

In this work, we measured the TPE spectrum of CF_2Cl_2 molecule within the photon energy range of 11.50–12.80 eV. According to the previous assignments, the contributions from two low-lying electronic states of $CF_2Cl_2^+$ cation, X^2B_2 and A^2A_2, were identified, in which the X^2B_2 band exhibited well-resolved vibrational structures. Using the ωB97XD density functionals with the cc-pVTZ base set, the geometries and vibrational frequencies of the CF_2Cl_2 neutral and cation in ground state were computed. The FC factors were then calculated for the possible vibrational transitions of $CF_2Cl_2(X^1A_1) \rightarrow CF_2Cl_2^+(X^2B_2)$. Based on the great agreement between the experimental and FC simulated spectra, the observed vibrational structures are well assigned. Interestingly, the threshold onset (11.755 eV) in the experimental spectrum is not the band origin of 0–0 transition as assigned in previous studies, and corresponds to the overtone excitation of $0 \rightarrow 5\nu_4^+$. Therefore, AIE of CF_2Cl_2 is corrected to 11.565 ± 0.010 eV, and the ν_1^+ and ν_4^+ frequencies of X^2B_2 are determined, too, according to our spectral assignment of the vibrational progression. In addition, the enthalpies of formation and C-Cl bond energies of CF_2Cl_2 neutral and cation are calculated with the aid of the present AIE and AP values.

The present study is a good example to show the application of FC simulation on accurate AIE measurement. Especially, when the molecular geometry is significantly changed in photoionization, the threshold onset might not correspond to the band origin of 0–0 transition. As shown in the recent investigations [13,43–48], this combined method of experimental TPE spectra and FC simulation not only provides a powerful tool to accurately determine ionization energy (IE) or electron affinity (EA) values, but also becomes a more effective strategy for assessing the reliability of computation methods.

CRediT authorship contribution statement

Hanhui Zhang: Methodology, Data curation, Writing - original draft. **Tongpo Yu:** Data curation, Visualization. **Xiangkun Wu:** Methodology. **Yan Chen:** Methodology. **Baokun Shan:** . **Xiaoguo Zhou:** Conceptualization, Writing - review & editing, Supervision, Funding acquisition. **Xinhua Dai:** Supervision, Funding acquisition. **Shilin Liu:** Supervision.

Declaration of Competing Interest

The authors declare that they have no known competing financial interests or personal relationships that could have appeared to influence the work reported in this paper.

Acknowledgement

This work was financially supported by the National Key Research and Development program of China (No. 2016YFF0200502), and the National Natural Science Foundation of China (No. 21903079, 21573210 and 21873089). X. Zhou also thanks the USTC-NSRL Association for financial support.

Appendix A. Supplementary material

Supplementary data to this article can be found online at https://doi.org/10.1016/j.cplett.2021.138631.

References

[1] B.J. Finlayson-Pitts, J.N. Pitts Jr, Chemistry of the upper and lower atmosphere: theory, experiments, and applications, Elsevier, 1999.
[2] S. Solomon, Stratospheric ozone depletion: A review of concepts and history, Rev. Geophys. 37 (3) (1999) 275–316.
[3] D.J. Jacob, Introduction to atmospheric chemistry, Princeton University Press, 1999.
[4] M.J. Molina, F.S. Rowland, Stratospheric sink for chlorofluoromethanes: chlorine atom-catalysed destruction of ozone, Nature 249 (5460) (1974) 810–812.
[5] D. Seccombe, R. Tuckett, F. Fisher, Fragmentation of the valence states of $CF_2Cl_2^+$, $CF_2H_2^+$, and CF_2Br^{2+} studied by threshold photoelectron–photoion coincidence spectroscopy, J. Chem. Phys. 114 (9) (2001) 4074–4088.
[6] J. Ajello, W. Huntress Jr, P. Rayermann, A photoionization mass spectrometer study of $CFCl_3$, CF_2Cl_2, and CF_3Cl, J. Chem. Phys. 64 (11) (1976) 4746–4754.
[7] H. Jochims, W. Lohr, H. Baumgärtel, Photoreactions of small organic molecules V. Absorption-, photoion-and resonancephotoelectron-spectra of CF_3Cl_2, CF_2Cl_2, $CFCl_3$ in the energy range 10–25 eV, Berichte der Bunsengesellschaft für physikalische Chemie 80 (2) (1976) 130–138.
[8] H. Schenk, H. Oertel, H. Baumgärtel, Photoreactions of small organic molecules VII photoionization studies on the ion-pair formation of the fluorochloromethanes CF_2Cl_2, CF_3Cl, and $CFCl_3$, Ber. Bunsenges. Phys. Chem. 83 (7) (1979) 683–691.
[9] R. Baker, J. Tate, Ionization and dissociation by electron impacf in CCl_2F_2 and in CCl_4 vapor, Phys. Rev. 53 (1938) 683.

[10] X. Wu, G. Tang, H. Zhang, X. Zhou, S. Liu, F. Liu, L. Sheng, B. Yan, Cl-Loss dynamics in the dissociative photoionization of CF_3Cl with threshold photoelectron–photoion coincidence imaging, Phys. Chem. Chem. Phys. 20 (7) (2018) 4917–4925.

[11] X. Wu, T. Yu, Y. Chen, X. Zhou, S. Liu, X. Dai, F. Liu, L. Sheng, Dissociative photoionization of CF_3Cl via the C_2E and D_2E states: competition of the C-F and C–Cl bond cleavages, Phys. Chem. Chem. Phys. 21 (9) (2019) 4998–5005.

[12] X.-K. Wu, X.-F. Tang, X.-G. Zhou, S.-L. Liu, Dissociation dynamics of energy-selected ions using threshold photoelectron-photoion coincidence velocity imaging, Chin. J. Chem. Phys. 32 (1) (2019) 11–22.

[13] Y. Chen, T. Yu, X. Wu, X. Zhou, S. Liu, F.-Y. Liu, X. Dai, C-F and C-H bond cleavage mechanisms of trifluoromethane ion in low-lying electronic states: threshold photoelectron-photoion coincidence imaging and theoretical investigations, Phys. Chem. Chem. Phys. 22 (2020) 13808.

[14] T. Pradeep, D. Shirley, High resolution photoelectron spectroscopy of CH_2F_2, CH_2Cl_2 and CF_2Cl_2 using supersonic molecular beams, J. Electron Spectrosc. Relat. Phenom. 66 (1–2) (1993) 125–138.

[15] T. Cvitaš, H. Güsten, L. Klasinc, Photoelectron spectra of chlorofluoromethanes, J. Chem. Phys. 67 (6) (1977) 2687–2691.

[16] R. Jadrny, L. Karlsson, L. Mattsson, K. Siegbahn, Valence electron spectra of the chlorofluoromethanes CF_3Cl, CF_2Cl_2 and $CFCl_3$, Phys. Scr. 16 (5–6) (1977) 235.

[17] J. Bunzli, D. Frost, F. Herring, C. McDowell, Assignment of the doublet states arising from ionization of chlorine lone-pairs in molecules possessing C2υ symmetry, J. Electron Spectrosc. Relat. Phenom. 9 (3) (1976) 289–305.

[18] X. Shan, X.J. Chen, L.X. Zhou, Z.J. Li, T. Liu, X.X. Xue, K.Z. Xu, High resolution electron momentum spectroscopy of dichlorodifluoromethane: Unambiguous assignments of outer valence molecular orbitals, J. Chem. Phys. 125 (15) (2006), 154307.

[19] C. Ning, X. Ren, J. Deng, G. Su, S. Zhang, F. Huang, G. Li, Investigation of outer valence orbital of CF_2Cl_2 by a new type of electron momentum spectrometer, Chin. Phys. 14 (12) (2005) 2467.

[20] D. Seccombe, R. Chim, R. Tuckett, H. Jochims, H. Baumgärtel, Vacuum–ultraviolet absorption and fluorescence spectroscopy of CF_2H_2, CF_2Cl_2, and CF_2Br_2 in the range 8–22 eV, J. Chem. Phys. 114 (9) (2001) 4058–4073.

[21] K. Takeshita, A theoretical study on the lonic states and the photoelectron spectra of dichlorodifluoromethane (CF_2Cl_2), J. Mol. Spectrosc. 142 (1) (1990) 1–9.

[22] M. Lewerenz, B. Nestmann, P.J. Bruna, S.D. Peyerimhoff, The electronic spectrum, photodecomposition and dissociative electron attachment of CF_2Cl_2: An ab initio configuration interaction study, J. Mol. Struct. (Thoechem.) 123 (3–4) (1985) 329–342.

[23] T. Liu, M.-B. Huang, H.-W. Xi, CASPT2 study on electronic states of the dichlorodifluoromethane cation, Chem. Phys. 332 (2–3) (2007) 277–283.

[24] T. Liu, W.-Z. Li, Q.-Z. Li, H.-F. Zhang, H.-W. Xi, Cl-loss and F-loss dissociations in low-lying electronic states of the $CF_2Cl_2^+$ ion studied using multiconfiguration second-order perturbation theory, Chem. Phys. Lett. 485 (4–6) (2010) 290–295.

[25] L. Sheng, F. Qi, H. Gao, Y. Zhang, S. Yu, W.-K. Li, Experimental and theoretical study of the photoionization and dissociative photoionizations of dichlorodifluoromethane, Int. J. Mass Spectrom. Ion Processes 161 (1–3) (1997) 151–159.

[26] K. Watanabe, T. Nakayama, J. Mottl, Ionization potentials of some molecules, J. Quant. Spectrosc. Radiat. Transfer 2 (4) (1962) 369–382.

[27] X. Tang, X. Zhou, M. Niu, S. Liu, J. Sun, X. Shan, F. Liu, L. Sheng, A threshold photoelectron-photoion coincidence spectrometer with double velocity imaging using synchrotron radiation, Rev. Sci. Instrum. 80 (11) (2009), 113101.

[28] B. Sztáray, T. Baer, Suppression of hot electrons in threshold photoelectron photoion coincidence spectroscopy using velocity focusing optics, Rev. Sci. Instrum. 74 (8) (2003) 3763–3768.

[29] J.-D. Chai, M. Head-Gordon, Long-range corrected hybrid density functionals with damped atom–atom dispersion corrections, Phys. Chem. Chem. Phys. 10 (44) (2008) 6615–6620.

[30] Y. Zhao, D.G. Truhlar, The M06 suite of density functionals for main group thermochemistry, thermochemical kinetics, noncovalent interactions, excited states, and transition elements: two new functionals and systematic testing of four M06-class functionals and 12 other functionals, Theor. Chem. Acc. 120 (1) (2008) 215–241.

[31] V.A. Mozhayskiy, A.I. Krylov, ezSpectrum, http://iopenshell.usc.edu/downloads.

[32] M.J. Frisch, G.W. Trucks, H.B. Schlegel, G.E. Scuseria, M.A. Robb, J.R. Cheeseman, G. Scalmani, V. Barone, G.A. Petersson, H. Nakatsuji, et al., Gaussian 16, revision C.01; Gaussian, Inc.: Wallingford, CT, 2016.

[33] J. Harvey, R.P. Tuckett, A. Bodi, A halomethane thermochemical network from iPEPICO experiments and quantum chemical calculations, J. Phys. Chem. A 116 (39) (2012) 9696–9705.

[34] B. Ruscic, D.H. Bross, Active Thermochemical Tables (ATcT) values based on ver. 1.122p of the Thermochemical Network (2020); available at ATcT.anl.gov.

[35] S.G. Lias, J.E. Bartmess, J.F. Liebman, J.L. Holmes, R.D. Levin, W.G. Mallard, J. Chem. Phys. Refrence Data 17, Suppl. No. 1 (1988).

[36] W. Griffiths, F. Harris, J. Barton, Experimental determination of the single-ionization energies of two environmentally important free radicals, $CF_2Cl^{\cdot}$ and $CFCl_2^{\cdot}$, Rapid Commun. Mass Spectrom. 3 (9) (1989) 283–285.

[37] Y.-L. He, L. Wang, Cations of halogenated methanes: adiabatic ionization energies, potential energy surfaces, and ion fragment appearance energies, Struct. Chem. 20 (3) (2009) 461–479.

[38] L. Leyland, J. Majer, J. Robb, Heat of formation of the $CF_2Cl^{\cdot}$ radical, Trans. Faraday Soc. 66 (1970) 898–900.

[39] S. Kumaran, K. Lim, J. Michael, A. Wagner, Thermal decomposition of CF_2Cl_2, J. Phys. Chem. 99 (21) (1995) 8673–8680.

[40] S. Kumaran, M.-C. Su, K. Lim, J. Michael, A. Wagner, Thermal decomposition of $CFCl_3$, J. Phys. Chem. 100 (18) (1996) 7533–7540.

[41] D. Seccombe, R. Chim, G. Jarvis, R. Tuckett, The use of threshold photoelectron–photoion coincidence spectroscopy to probe the spectroscopic and dynamic properties of the valence states of CCl_3F^+, CCl_3H^+ and CCl_3Br^+, Phys. Chem. Chem. Phys. 2 (4) (2000) 769–780.

[42] S. Kumaran, M.-C. Su, K. Lim, J. Michael, A. Wagner, L.B. Harding, D.A. Dixon, Ab initio calculations and three different applications of unimolecular rate theory for the dissociations of CCl_4, $CFCl_3$, CF_2Cl_2, and CF_3Cl, J. Phys. Chem. 100 (18) (1996) 7541–7549.

[43] H. Zhang, W. Cao, Q. Yuan, X. Zhou, M. Valiev, S.R. Kass, X.-B. Wang, Cryogenic "iodide-tagging" photoelectron spectroscopy: a sensitive probe for specific binding sites of amino acids, J. Phys. Chem. Lett. 11 (11) (2020) 4346–4352.

[44] T. Yu, X. Wu, X. Zhou, A. Bodi, P. Hemberger, Hydrogen migration as a potential driving force in the thermal decomposition of dimethoxymethane: New insights from pyrolysis imaging photoelectron photoion coincidence spectroscopy and computations, Combust. Flame 222 (2020) 123–132.

[45] X. Wu, X. Zhou, P. Hemberger, A. Bodi, Conformers, electronic states, and diabolical conical intersections in the valence photoelectron spectroscopy of halocyclohexanes, J. Chem. Phys. 153 (5) (2020), 054305.

[46] X. Wu, X. Zhou, P. Hemberger, A. Bodi, A guinea pig for conformer selectivity and mechanistic insights into dissociative ionization by photoelectron photoion coincidence: fluorocyclohexane, Phys. Chem. Chem. Phys. 22 (4) (2020) 2351–2360.

[47] L. Wang, Q. Yuan, W. Cao, J. Han, X. Zhou, S. Liu, X.-B. Wang, Probing orientation-specific charge-dipole interactions between hexafluoroisopropanol and halides: a joint photoelectron spectroscopy and theoretical study, J. Phys. Chem. A 124 (10) (2020) 2036–2045.

[48] L. Wang, J. Han, Q. Yuan, W. Cao, X. Zhou, S. Liu, X.-B. Wang, Electron affinity and electronic structure of hexafluoroacetone (HFA) revealed by photodetaching the $[HFA]^{\bullet-}$ radical anion, J. Phys. Chem. A (2020).